

PACS numbers: 42.25.Bs; 47.70.Pq; 82.33.Ux
DOI: 10.1070/QE2012v042n04ABEH014812

Absorption and scattering of laser radiation by the diffusion flame of aviation kerosene

S.V. Gvozdev, A.F. Glova, V.Yu. Dubrovskii, S.T. Durmanov, A.G. Krasyukov, A.Yu. Lysikov, G.V. Smirnov, V.B. Solomakhin

Abstract. **The absorption coefficient of the radiation of a repetitively pulsed Nd:YAG laser with an average output power up to 6 W and of a cw ytterbium optical fibre laser with an output power up to 3 kW was measured in the diffusion flame of aviation kerosene burning on a free surface in the atmospheric air. The absorption coefficient as a function of flame length, radiation power, and radiation intensity, which was varied in the $\sim 10^3 - 5\times 10^4$ W cm^{-2} range, was obtained for two distances (1 and 2 cm) between the laser beam axis and the surface. The coefficient of radiation absorption by kerosene flame was compared with that in ethanol and kerosene–ethanol mixture flames. The radiation power scattered by a small segment of the kerosene flame irradiated by Nd:YAG laser radiation was measured as a function of longitudinal and azimuthal coordinates. An estimate was made of the total scattered radiation power.**

Keywords: *flame, laser, radiation intensity, absorption coefficient, scattering.*

1. Introduction

The use of laser radiation for igniting gaseous and condensed media and for exerting influence upon a flame is of scientific and practical interest. This is due to the possibility of investigating inflammation conditions [1–3] and the capability of controlling combustion regimes [4–6] with the help of a local energy source with well-known and controllable parameters, which may be formed remotely in an arbitrary region of the object under investigation.

The interaction of a flame with the laser radiation of sufficiently high intensity may be self-consistent: variations of the total power and intensity due to absorption, scattering, and refraction of the radiation exert effect on flame characteristics, whose variation in turn affects the radiation parameters. A similar feedback also exists, for instance, in the interaction of laser radiation with the plasma of an optical gas discharge [7]. However, the complex chemical and aggregate composition of the majority of flames [8] and a strong temperature dependence of chemical reaction rates [9] in flames may give rise to a feedback for substantially lower intensities than in the case of an optical gas discharge.

Clearly the measure of the effect of a flame on radiation parameters will be determined by the kind and size of the flame as well as by the fuel type. In our view, this subject has not received adequate attention in the literature. This problem may arise, for instance, when a laser is employed for remote cutting of metal structures of dangerous oil or gas wells [10]. Under these conditions there is no way of executing any quantitative measurements, and the only way of obtaining the required information involves model laboratory experiments. The selection of fuel for these experiments is not unambiguous, because the initial chemical composition of the mixture burning in an oil or gas well accident is, as a rule, unknown due to a variety of accompanying products. In certain cases, the hydrocarbon flame of aviation kerosene may be an approximation to the composition of such burning mixtures.

The objective of our work is to experimentally investigate the absorption and scattering of laser radiation with a wavelength $\lambda \approx 1$ μm by the diffusion flame of aviation kerosene burning on a free surface in the atmospheric air and to compare the absorption coefficient of this radiation with that for ethanol and ethanol–kerosene mixtures.

2. Experimental facility and measurement techniques

Our facility is schematically represented in Fig. 1. The radiation of a repetitively pulsed (RP) Nd:YAG laser ($\lambda = 1.06$ μm, a half-amplitude pulse duration $\tau = 130$ μs, a pulse-repetition rate $f = 1 - 50$ Hz, a highest pulse energy of 0.5 J) or a cw ytterbium fibre laser ($\lambda = 1.07$ μm, a peak power of 4 kW) (*1*) is collimated using lenses (*2*) and (*3*) into a laser beam, which may be treated as parallel over the length of the flame region (*4*). The beam diameter d can be varied by adjusting the collimator. It was assumed to be equal to the size of beam imprint on the surface of a material with a low thermal conductivity coefficient under short-term laser switching, or to the size of a hole burned in a Teflon film, which yielded close results. A power meter (*7*) (a Nova model with a measurement uncertainty of ±5%) served to measure the radiation power with and without the flame, which allowed measuring the power loss in the radiation passage through the flame. The scattered radiation power was measured with an FD-21 KP photodiode (*14*) mounted, together with a set of elements (*8–13*), on an optical bench pivotable about a point O. Elements (*9*) and (*10*), which are mounted on the bench, as

S.V. Gvozdev, A.F. Glova, V.Yu. Dubrovskii, S.T. Durmanov, A.G. Krasyukov, A.Yu. Lysikov, G.V. Smirnov State Research Centre of Russian Federation 'Troitsk Institute for Innovation and Fusion Research' (TRINITI), bldg 12, ul. Pushkovykh, 142190 Troitsk, Moscow region, Russia; e-mail: afglova@triniti.ru;
V.B. Solomakhin Gazprom Gazobezopasnost, POB 128, bldg 1, ul. Stroitelei 8, 119311 Moscow, Russia

Received 23 December 2011, revised 14 February 2012
Kvantovaya Elektronika **42** (4) 350–354 (2012)
Translated by E.N. Ragozin

well as plate (*6*) are employed in the calibration of the photodiode and are removed from the setup during measurements. The aperture stop (*8*) 4 mm in diameter is used to separate out the radiation scattered from a small flame segment. Rotating the bench about the axis *O* permits measuring the power of this radiation in relation to the scattering angle, while translating the flame cell along the beam axis for a fixed angle yields the radiation power scattered by different flame segments. In the rotation of the bench, the centre of preferred flame segment was bound to the centre of the aperture stop (*8*) by shifting the flame cell, while the variations of the visible segment length arising from the rotations were taken into account with the help of a geometrical factor calculated for the known facility dimensions.

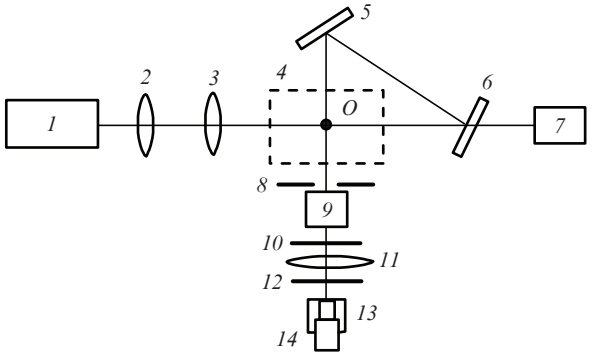

Figure 1. Layout of the facility: (*1*) cw fibre or RP Nd:YAG laser; (*2*, *3*) collimator lenses; (*4*) flame region; (*5*, *6*) radiation-attenuating plates; (*7*, *9*) radiation detectors; (*8*) aperture stop; (*10*) set of neutral density light filters; (*11*) shaping lens; (*12*) IR light filter; (*13*) light shield; (*14*) photodiode.

The flame was initiated by igniting in the air the vapour of a combustible liquid, which filled the cell of three similar 20-mm wide sections of length 50 mm along the beam; the sections were separated by 2-mm thick walls. The flame length along the beam axis was varied by changing the number of sections with the liquid set on fire. Use was made of the flame of TS-1 aviation kerosene, ethanol, and kerosene–ethanol mixtures. The quiet flame of kerosene burning in one section has the appearance of the diffusion hydrocarbon flame of a Bunsen burner [8]: a ~1.5-cm high clearly defined inner cone of light blue colour is surrounded by a yellow diffusion region, which passes with height (~10 cm) into a region of intense carbon-black formation. All measurements were made with quiet flames. The flame was stabilised due to protective walls with windows for the input and output of radiation, which surrounded the flame on four sides and did not prevent the inflow of air into combustion region.

3. Results and their discussion

3.1. Radiation scattering

Measurements of the radiation power scattered by the flame were made in its propagation through the yellow part of the kerosene flame of length l =4.5 cm for a distance h = 2 cm of the beam axis from the cell edge. For a radiation source we employed a RP Nd:YAG laser with a pulse repetition rate f = 15 Hz; the laser beam diameter d = 5.5 mm. The average radiation power at the flame input, the pulsed input power and intensity were fixed and were equal to $\langle P_{in}\rangle = 2.5$ W, $P_{in}^{p} = \langle P_{in}\rangle/(f\tau) = 1280$ W, and $I_{in}^{p} = P_{in}^{p}/S \approx 4\times10^{3}$ W cm^{-2}, respectively (here, $S = \pi d^2/4$).

Under these values of the intensity and the spacing h, the radiation–flame interaction is attended with a glow of the beam path and the emergence of a characteristic sound with a pulse repetition rate. This may arise from additional heating and laser-field-induced intense combustion of the particles located in this part of the flame. Irrespective of their nature and production mechanism [5], the scattering of laser radiation by the flame is primarily due to these particles.

Figure 2 depicts the dependence of the scattered radiation power W, separated out by the aperture of the lens (*11*) and measured with an accuracy of ±15%, on the scattering angle φ and on the displacement X of the front edge of the flame relative to the centre of the aperture stop (*8*) towards the beam. In this case, $X = 0$ corresponds to the front edge of the flame, $\varphi = 90°$ corresponds to the mutually orthogonal orientation of the axes of the laser beam and the bench with the photodiode, and $\varphi = 70°$ and 110° correspond to 20° rotations of the bench axis towards the beam and in the opposite direction, respectively. Similar dependences were obtained for other values of φ not shown in Fig. 2. One can see from Fig. 2 that the scattering is anisotropic. A qualitative explanation can be provided only to the lowering of scattered radiation power in comparison with the radiation power scattered at the front edge of the flame, which takes place with increase in X for all angles φ because of the absorption of radiation in its propagation through the flame. Explaining other features of the scattering invites numerical simulations with the inclusion of data about the sort, density, and size distribution of the particles as well as about their size variation rate during combustion [11].

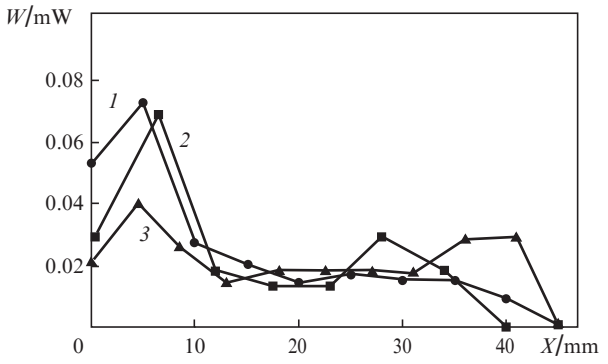

Figure 2. Radiation power W scattered by kerosene flame, which is separated out by the aperture of lens (*11*), as a function of displacement X for scattering angles $\varphi = 90°$ (*1*), 70° (*2*), and 110° (*3*), $\langle P_{in}\rangle = 2.5$ W, f = 15 Hz, d = 5.5 mm, h = 2 cm, l = 4.5 cm.

We take advantage of the data given in Fig. 2 to estimate the total scattered radiation power. The scattering is assumed to be isotropic and similar for all flame segments of length $x = 5$ for $\varphi = 90°$ formed by the aperture stop (*8*). For the total scattered radiation power W_Σ and its fraction δ relative to P_{in}^{p} we have $W_\Sigma = W_1 N(4\pi/\Omega) = 3$ W and $\delta = W_\Sigma/P_{in}^{p} = 0.23\%$, where $W_1 = 0.022$ mW is the average radiation power scattered by each segment of length x, which was

obtained from Fig. 2; $N = l/x$ is the number of segments; $\Omega = 8.3\times10^{-4}$ sr is the solid angle at which the lens (*11*) (with an aperture of 2 cm and a lens–flame separation of 61.5 cm) is seen from the centre of a segment. We note that the above estimates for W_Σ and δ are upper estimates, since they do not take into account the increase in spectral energy brightness of the flame at $\lambda = 1$ μm arising from the temperature increase due to laser-induced particle heating. By taking into account the certified parameters of the photodiode in use it is possible to show [12] that an increase in kerosene flame temperature from the value ~900 °C, which is typical for combustion in the air, to, for instance, 1500 °C results in about a 30% rise of the photodiode signal unrelated to the radiation scattering.

3.2. Radiation absorption

A lowering of the average radiation power $\langle P_{out}\rangle$ of the RP laser at the flame output caused the absorption and scattering of the radiation may be described by the expression $\langle P_{out}\rangle = \langle P_{in}\rangle(1 - R)\exp(-\alpha l)$, where R is the effective scattered radiation fraction and α is the absorption coefficient averaged over the flame length l. Putting $R \approx \delta$, in view of the resultant estimate $\delta = 0.23\%$ we assume that $R \approx 0$ and for the average absorption coefficient of the RP laser radiation we have the expression $\alpha = -(1/l)\ln(\langle P_{out}\rangle/\langle P_{in}\rangle)$. The magnitude of R for the cw laser radiation is also assumed to be approximately equal to δ, and on replacing $\langle P_{in}\rangle$ with P_{in} and $\langle P_{out}\rangle$ with P_{out} we obtain a similar expression for the radiation absorption coefficient, where P_{in} and P_{out} are the input and output powers of the cw radiation, respectively.

In this Section we outline the α measurement data, which rely on the above formula, in relation to flame and laser radiation parameters. All measurements were made for the transversely central part of the flame. The measurement uncertainty was ±10%. We observed no noticeable change of the beam diameter in the course of beam propagation through the flame. This permits neglecting the effect of radiation refraction on the intensity.

Table 1 shows the absorption coefficients α in relation to l, h, and $\langle P_{in}\rangle$ upon irradiation of kerosene flame by the RP Nd:YAG laser pulses. The radiation intensity I_{in}^{p} at the flame input was about the same for all irradiation regimes and was equal to $(2 - 5)\times10^3$ W cm^{-2}. The dependence of α on l for a given h persists for other values of the length, and Table 1 gives the values of α only for two approximately equal lengths and for two values of h. The input power was varied by changing the pulse repetition rate for a fixed pump power. The values of f and d corresponding to a given power $\langle P_{in}\rangle$ are indicated in the heading of Table 1 in brackets.

The data collected in Table 1 possess three main features. First, the absorption coefficient is independent of the input power. This is due to the convective motion of the medium and the products of its interaction with the radiation, with the consequential complete renewal of a medium volume of size d during the interpulse period, so that the next radiation pulse interacts with the same medium as the previous pulse. Specifically, for a characteristic medium motion velocity $v \sim 1$ m s^{-1} [9] the period of its renewal for $d \sim 5$ mm is $d/v \sim 5$ ms, which is much shorter than the minimal interpulse period $\sim 1/f = 20$ ms for $f = 50$ Hz. Second, the absorption coefficient depends on the flame length, and with its increase it becomes stronger in the blue region of the flame ($h = 1$ cm) and shows a tendency for a decrease in the yellow region ($h = 2$ cm). Third, for equal lengths the absorption coefficient in the blue flame region is lower than in the yellow one. The two last-named features are attributable to the variation of flame composition with height.

In the blue region, because of the low density of solid particles the interaction takes place primarily with the gaseous medium. Here, it is possible to neglect the radiation power loss arising from the interaction with particles, with the exception of losses in the narrow zone of the curved front edge of the flame [9, 11], and if there are no strong absorption bands at $\lambda = 1.06$ μm, the absorption coefficient will be lower than in the yellow region. The lowering of α in the yellow region of the flame with increase in its length is related to radiation absorption by the gaseous products of particle combustion: as the radiation is attenuated with length, the rate of additional product generation in the heating of particles under laser irradiation becomes lower, and therefore the length-averaged absorption coefficient becomes smaller. To interpret the effect of the increase in α with length in the blue region of the flame we assume that the polarisation of molecules in the laser radiation field results in their clustering, and these clusters may have absorption bands corresponding to the radiation wavelength. Since the total number of clusters rises with length and their structure changes owing to the lowering of the radiation field, α may also exhibit a change, including an increase.

In addition to combustion intensification under particle heating, the action of laser radiation may lead to dissociation of gaseous combustion products. If it is assumed that the absorption bands of dissociation products are less intense than those of the initial combustion products and in some of dissociation products are missing at all, one would expect a lowering of α with increase in I_{in}^{p}, because the degree of dissociation increases with increasing I_{in}^{p}. This assumption corresponds to the measurement data presented in Fig. 3.

On analysing the data given in Table 1 and Fig. 3 we note that a better substantiated interpretation of the dependences of α on l, h, and I_{in}^{p} could be provided with the help of near-IR absorption spectra of kerosene flame, but we failed to find them in the literature.

We compare the measured α data for the RP Nd:YAG laser radiation and $h = 2$ cm with the data for the cw fibre

Table 1. Absorption coefficients α (cm^{-1}) upon irradiation of kerosene flame by RP Nd:YAG laser pulses for $I_{in}^{p} \approx (2-5)\times10^3$ W cm^{-2}.

h/cm	l/cm	$\langle P_{in}\rangle$/W (f/Hz; d/mm)			
		0.6 (5; 5.5)	2.4 (15; 5.5)	3.8 (25; 6.3)	6.2 (50; 7.5)
1	3.5–4	0.015	–	0.015	0.015
	11	0.029	–	0.026	0.026
2	2.5–3	0.064	0.066	–	0.062
	9–11	0.054	0.053	–	0.051

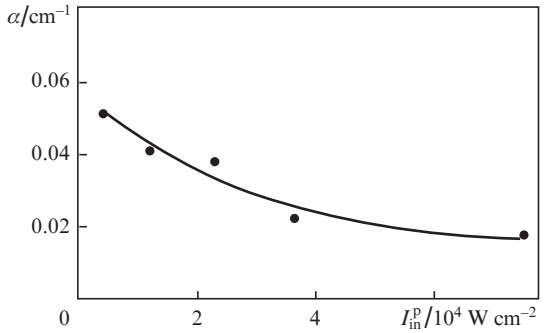

Figure 3. Dependence of α on I_{in}^{p} for kerosene flame for $\langle P_{in}\rangle = 2.7$ W, $f = 15$ Hz, $h = 2$ cm, and $l \approx 9$ cm.

laser and the same h value for kerosene flame, which are collected in Table 2. In the execution of measurements with this laser, the highest radiation intensity I_{in} at the flame input was close to I_{in}^{p} and approximately corresponded to the intensities typically used in the remote cutting of metals by cw laser radiation [13, 14]. One can see from Table 2 that the absorption coefficient for the cw laser radiation, like for the RP laser radiation, lowers with increase in flame length. However, for close intensities ($I_{in} \sim I_{in}^{p} \sim 10^3$ W cm^{-3}) for both lasers and lengths it is significantly higher than for the RP laser. The greater α value for the cw laser radiation is attributable to the fact that the average temperature of the in-flame heated particles will be higher under the additional cw radiation heating than under RP radiation heating. As a consequence, the density of radiation-absorbing combustion products will be higher to result in a greater α. The increase in combustion product density with temperature may also explain the rise in α with increasing I_{in} for invariable input power and flame length, when the intensity was made higher by shortening the beam diameter (see the lines for $P_{in} = 100$ and 950 W in Table 2). It is pertinent to note that the rise in α with increasing I_{in} in the range of I_{in} variation investigated for the cw laser is exactly the opposite of the α lowering with increasing I_{in}^{p} for the RP laser depicted in Fig. 3. The reason is that the increase in absorption with increase in density of combustion products prevails over absorption lowering arising from their dissociation for a moderate (~10^3 W cm^{-2}) highest intensity of the cw radiation.

Also worthy of note is the growth of α with increasing P_{in} for a fixed flame length l and a nearly constant intensity $I_{in} \approx 10^3$ W cm^{-2}. This effect is supposedly due to the fact that the heat source above the burning liquid surface, which is formed by the radiation power released in the flame, exerts effect on the liquid evaporation rate, this effect becoming progressively stronger with increasing power. As a result, the density of the consequently produced particles also increases to entail a rise in absorption coefficient.

Table 2. Absorption coefficients α (cm^{-1}) upon irradiation of kerosene flame by cw fibre laser radiation ($h = 2$ cm).

P_{in}/W	d/mm	I_{in}/W cm^{-2}	l/cm		
			3.5	8	13
100	3	1.4×10^3	–	0.117	0.078
	8	1.9×10^2	0.114	0.074	0.07
950	8	1.8×10^3	0.23	0.132	0.121
	15	5.5×10^2	0.145	0.13	0.116
3000	15	1.7×10^3	–	0.32	0.24

Table 3. Absorption coefficients upon irradiation of ethanol–kerosene mixture flame by the RP Nd:YAG laser pulses for $\langle P_{in}\rangle = 2.8$ W, $f = 15$ Hz, $d = 2$ mm, $\langle I_{in}^{p}\rangle = 4.6\times10^4$ W cm^{-2}, $h = 2$ cm, $l = 13$ cm.

α/cm^{-1}	Ethanol fraction (%)
0.026	0
0.015	20
0.0072	50
0.0036	80
0.0014 (0.0016)	100

Note. Given in parentheses is the value of for the radiation of the cw fibre laser for $P_{in} = 970$ W, $d = 8$ mm, $I_{in} = 1.8\times10^3$ W cm^{-2}, $h = 2$ cm, $l = 13$ cm.

We next compare the absorption coefficient measurement data for kerosene flame and ethanol and kerosene–ethanol mixture flames. In going over to these flames we endeavoured to change the initial composition of combustion mixture, whose flame interacts with intense laser radiation. The measurements with the mixtures were made during the first 30 s after initiating flame in the cell. This was because of the burnout of ethanol in the mixture, which had an appreciably lower vaporisation temperature than kerosene. The absorption coefficient of the mixture flames was measured for the RP Nd:YAG laser radiation, and that of ethanol was measured for the radiation of the RP Nd:YAG and cw fibre lasers.

The measurement data are collected in Table 3. One can see that the absorption coefficient of ethanol flame is independent of the laser operation regime and the radiation intensity. This is due to the absence of hot solid particles in the flame, as witnessed by the blue colour of the flame throughout its length. The radiation absorption coefficient of ethanol flame is significantly lower than that of kerosene flame and is defined by one of combustion products, namely by water vapour [15]. The absorption coefficient rises with lowering the fraction of ethanol. Simultaneously changed is the flame appearance: the emerging yellow region with heated particles, which are responsible for the bulk of radiation absorption, becomes progressively more pronounced.

4. Conclusions

Our measurements showed that the fraction of 1-μm laser radiation scattered by the diffusion flame of aviation kerosene is low and amounts to a fraction of one percent. The radiation absorption coefficient of this flame depends on the flame length, the radiation intensity, the laser operation mode, and the flame region through which the radiation propagates. The absorption of radiation with an intensity of $10^3 - 10^4$ W cm^{-2} in the flame depends on the type of fuel and may vary over a broad range. The resultant data may be an aid in the selection of radiation parameters and the site of a high-power laser facility intended for operation on a dangerous oil or gas well.

Acknowledgements. This work was supported by Gazprom Gazobezopasnost.

References

1. Vorontsov S.S., Zudov V.N., Tret'yakov P.K., Tupikin A.V. *Teplofizika i Aeromekhanika*, **13**, 667 (2006).
2. Kazantsev S.Yu., Kononov I.G., Kossyi I.A., Tarasova N.M., Firsov K.N. *Fiz. Plazmy*, **35**, 281 (2009).
3. Vysokomornaya O.V., Kuznetsov G.V., Strizhak P.A. *Teplovye Protsessy v Tekhnik*e, **3**, 113 (2011).
4. Kozlov G.I., Kuznetsov V.A., Sokurenko A.D. *Pis'ma Zh. Tekh. Fiz*., **16**, 55 (1990).
5. Li Ch.B., Li V., O K.Ch., Shin Kh.D., En D.-K. *Fizika Goreniya i Vzryva*, **42**, 74 (2006).
6. Vorontsov S.S., Tret'yakov P.K., Tupikin A.V. *Khim. Fiz.*, **29**, 53 (2010).
7. Raizer Yu.P. *Fizika gazovogo razryada* (The Physics of a Gas Discharge) (Moscow: Nauka, 1987).
8. Gaydon A.G. *The Spectroscopy of Flames* (London: Chapman and Hall, 1957, 1974; Moscow: IL, 1959).
9. Frank-Kamenetskii D.A. *Diffuziya i teploperedacha v khimicheskoi kinetike* (Diffusion and Heat Transfer in Chemical Kinetics) (Moscow: Nauka, 1987).
10. Blokhin O.A., Vostrikov V.G., Gavrilyuk V.D., et al. *Khimicheskoe i Neftegazovoe Mashinostroenie*, (5), 52 (2001).
11. Khitrin A.N. *Fizika goreniya i vzryva* (The Physics of Combustion and Explosion) (Moscow: Izd. MGU, (1957).
12. Lebedeva V.V. *Tekhnika opticheskoi spektroskopii* (Techniques of Optical Spectroscopy) (Moscow: Izd. MGU, (1977).
13. Likhanskii V.V., Loboiko A.I., Antonova G.F., Krasyukov A.G., Sayapin V.P. *Kvantovaya Elektron.*, **26**, 139 (1999) [*Quantum Electron.*, **29**, 139 (1999)].
14. Antonova G.F., Gladush G.G., Krasyukov A.G., Kosyrev F.K., Rodionov N.B. *Teplofiz. Vys. Temp*., **38**, 501 (2000).
15. Measures R. *Laser Remote Sensing* (New York: Wiley: 1984; Moscow: Mir, 1987).